Quench protection performance measurements in the first MQXF magnet models

E. Ravaioli, G. Ambrosio, H. Bajas, G. Chlachidze, A. Fernandez Navarro, P. Ferracin, S. Izquierdo Bermudez, P. Joshi, J. Muratore, F. Rodriguez-Mateos, GL. Sabbi, S. Stoynev, E. Todesco, and A. Verweij

***Abstract*—CERN and US LARP (LHC Accelerator Research Program) are jointly developing Nb_3Sn quadrupole magnets to be installed in the LHC for its upgrade to higher luminosity. These magnets' quench protection system will include a combination of quench heaters attached to the coil surfaces and CLIQ units electrically connected to the magnets. Different protection elements have been characterized separately and simultaneously by implementing them on two 1.2 meter long model quadrupole magnets, tested at FNAL and CERN, and one 4.0 meter long mirror magnet tested at BNL. After analyzing the test data, their performances have been positively evaluated. Furthermore, the electro-thermal transients occurring after a quench have been simulated with the LEDET software and the results compared to experimental results. The preferred quench protection system configuration relies both on heaters and CLIQ. This solution is based on electrically robust components, achieves an effective reduction of the coils hot-spot temperature after a quench, and offers increased redundancy against component failures.**

***Index Terms*—accelerator magnet, circuit modeling, CLIQ, quench protection, superconducting coil.**

I. Introduction

ACHIEVING the targets of the High Luminosity LHC project requires the replacement of the superconducting quadrupole magnet system adjacent to the two high-luminosity interaction regions, ATLAS and CMS [1]–[3]. This system, often referred to as inner triplet, will be composed of four separate electrical circuits, each including six 150 mm aperture, two-layer, Nb_3Sn quadrupole magnets (MQXF), four of which with a magnetic length of 4.2 m (MQXFA) and two of 7.15 m (MQXFB) [4]–[7]. The main parameters of these magnets are summarized in Table I [4], [7], [8], and its magnetic field map in one half pole is shown in Fig. 1a. The peak magnetic field in the conductor approaches 12 T.

Protecting these magnets against the effects of a quench is challenging due to the high magnetic-energy density stored in the coils [9]–[13]. An effective and fast heating mechanism is required to transfer most of the coil to the normal state in a few tens of millisecond, thus quickly discharging the magnet current and depositing the stored energy more uniformly in the winding pack. Furthermore, the quench protection system must depend on robust and reliable components to minimize the risk of a long LHC shut-down.

The inner triplet quench protection system relies on heaters and Coupling-Loss Induced Quench (CLIQ) technologies [14]–[16]. Heaters are μm-thick stainless-steel strips glued to the coils' surfaces and separated from the conductor by a thin insulation layer. Upon quench detection, current is driven through them to heat them up and transfer energy to the coil via thermal diffusion. The designs of the

TABLE I
Main Magnet and Conductor Parameters [4], [7], [8].

Parameter	Unit	MQXFA	MQXFB
Nominal current, I_{nom}	A	16471	
Ultimate current, I_{ult}	A	17800	
Peak field in the conductor at I_{nom}	T	11.4	
Operating temperature	K	1.9	
Magnetic length, l_{m}	m	4.20	7.15
Differential inductance at I_{nom}	mH	34.4	58.6
Stored energy at I_{nom}	MJ	4.7	7.9
Number of turns per pole, outer layer	-	28	
Number of turns per pole, inner layer	-	22	
Superconductor composition	-	Ti-alloyed Nb_3Sn	
Number of strands	-	40	
Strand diameter, d_s	mm	0.85	
Bare cable width	mm	18.363	
Bare cable thickness	mm	1.594	
Insulation thickness	mm	0.145	
Copper/non-Copper ratio	-	1.15	
Filament twist pitch, $l_{\mathrm{tp,f}}$	mm	19	
Strand twist pitch, $l_{\mathrm{tp,s}}$	mm	109	
RRR of the copper matrix	-	200	

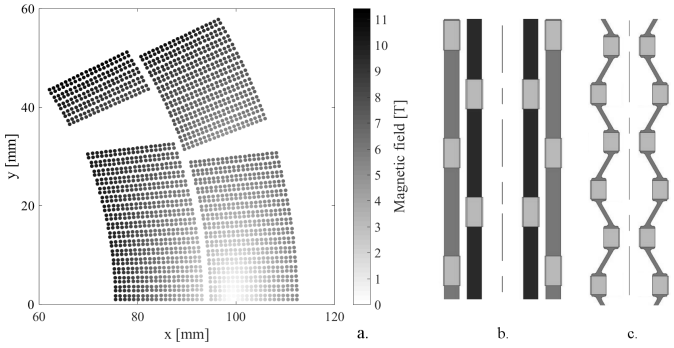

Fig. 1. High Luminosity LHC Nb_3Sn quadrupole magnet [9]. a. Cross-section of one half pole, showing the magnetic field at the nominal current of 16.47 kA. b. Heater strip traces attached to the coil's outer layer (OL-H). c. Heater strip traces attached to the coil's inner layer (IL-H). Darker gray sections indicate Cu-plated regions.

Work supported by the US Department of Energy through the US LHC Accelerator Research Program (LARP) and NSFC (Contract No. 11427904).

E. Ravaioli and GL. Sabbi are with the Lawrence Berkeley National Laboratory, Berkeley, CA. (e-mail: ERavaioli@lbl.gov).

G. Ambrosio, G. Chlachidze, and S. Stoynev are with the Fermilab National Accelerator Laboratory, Batavia, IL.

H. Bajas, A. Fernandez Navarro, P. Ferracin, S. Izquierdo Bermudez, F. Rodriguez-Mateos, E. Todesco, and A. Verweij are with CERN, Geneva, CH.

P. Joshi and J. Muratore are with Brookhaven National Laboratory, Upton, NY.

Manuscript received August 29, 2017.

TABLE II
MQXF HEATER PARAMETERS.

Parameter	Unit	MQXFA		MQXFB	
		OL-H	IL-H	OL-H	IL-H
l_{H}	m	4.2	4.2	7.0	7.0
N_{hs}	-	26	65	45	110
R_{hs}	mΩ	27	44	27	44
R_{w}	Ω	0.6	0.6	0.6	0.6
R_{H}	Ω	2.9	4.2	4.6	6.7
U_{H}	V	570	565	900	900
C_{H}	mF	7.05	7.05	7.05	7.05
I_{H}	A	198	134	198	134
τ_{H}	ms	20	30	32	47
P_{H}	Wcm^{-2}	213	98	213	98
E_{H}	Jcm^{-2}	2.16	1.45	3.42	2.32

heater strips attached to the MQXF coil's outer (OL-H) and inner layer (IL-H) are shown in Fig. 1b and 1c, respectively. CLIQ is a recently-developed method to heat up the coil by utilizing coupling loss. It relies on capacitive units that are connected to the coils to protect and are discharged upon quench detection, hence introducing fast current changes in the coil sections. The resulting local magnetic-field change generates high inter-filament coupling loss [17], [18], which heats the copper matrix of the strands. The units are composed of simple, reliable, easy to repair electrical elements. CLIQ technology has been tested on magnets of different geometries, superconductor types, and sizes [16], [19]–[22], including full-scale accelerator magnets [23], [24].

In order to assess the performance of the quench protection system in conditions similar to the design targets, experimental campaigns have been carried out at the magnet test facilities of the Brookhaven Nation Laboratory (BNL) [25], European Organization for Nuclear Research (CERN) [26]–[28], and Fermi National Acceleration Laboratory (FNAL) [29]–[31].

Magnet discharges reproducing LHC relevant conditions were performed and compared to simulation results obtained with the LEDET (Lumped-Element Dynamic Electro-Thermal) program [14], [32], [33].

II. QUENCH PROTECTION SYSTEM ELEMENTS

The inner-triplet quench protection system includes heaters attached to the coils' surfaces and CLIQ units electrically connected to the magnets via dedicated current leads.

A. Heaters

Each magnet is equipped with 16 OL-H and 8 IL-H strips [10]. Heater strips are connected in pairs to units including a capacitor bank of capacitance C_{H} [F] charged to a voltage U_{H} [V]. The strip lengths l_{H} [m], numbers and resistances of heating stations N_{hs} and R_{hs} [Ω], and room-temperature wiring resistances R_{w} [Ω] are reported in Table II, together with the resulting total heater circuit resistances $R_{\mathrm{H}}{=}2N_{\mathrm{hs}}R_{\mathrm{hs}}{+}R_{\mathrm{w}}$, and peak currents $I_{\mathrm{H}}{=}U_{\mathrm{H}}/R_{\mathrm{H}}$. For each design, the peak power density deposited in the heating stations can be calculated as $P_{\mathrm{H}}{=}R_{\mathrm{hs}}I_{\mathrm{H}}^2/S_{\mathrm{hs}}$ [Wm^{-2}], with S_{hs} [m^2] the contact surface between one heating station and the coil. In first approximation, the heater current decays exponentially with time constant $\tau_{\mathrm{H}}{=}R_{\mathrm{H}}C_{\mathrm{H}}$ [s]. Hence, the total energy density deposited during decay can be calculated as $E_{\mathrm{H}}{\approx}P_{\mathrm{H}}\tau_{\mathrm{H}}/2$ [Jm^{-2}]. The outer-layer heaters are designed to reach higher P_{H} and E_{H} than the inner-layer heaters, since they are attached to coil regions with lower magnetic field where higher energy deposition is required to quench. The same type of heater unit is used to power MQXFA and MQXFB strips in order to reduce the number of required spare units. The units connected to MQXFA shorter, less resistive heater strips will be charged to a lower voltage to limit the peak heater current to the same value as MQXFB strips. As a consequence, the same P_{H} is achieved in the strips of both magnet types, but the time-constant and energy density deposited in MQXFA strips are smaller.

TABLE III
MQXF HEATER-DELAY TEST PEAK POWER AND ENERGY DENSITY.

Parameter	Unit	LF-OL-H	HF-OL-H	IL-H
P_{H}, MQXFS1	Wcm^{-2}	213	213	98
P_{H}, MQXFS3	Wcm^{-2}	123	123	122
P_{H}, MQXFPM1	Wcm^{-2}	179	192	83
E_{H}, MQXFS1	Jcm^{-2}	3.44	3.42	2.33
E_{H}, MQXFS3	Jcm^{-2}	2.60	2.60	2.59
E_{H}, MQXFPM1	Jcm^{-2}	2.75	2.85	1.88

A key parameter for defining heater performance is the heater delay, defined as the time between the heater unit triggering and the onset of the induced coil transition to the normal state. Heater delays of selected heater strips are tested on two 1.2 m long quadrupole magnets (MQXFS1, MQXFS3) [26]–[30] and one 4.0 m long mirror magnet (MQXFPM1) [25]. The heater circuits parameters selected during the three test campaigns, reported in Table III, are set as similar as possible to the MQXFB design, compatibly with the hardware limitations in the magnet test facilities.

The delays measured after powering strips connected to the coils' outer layers are plotted in Fig. 2a. As expected, the delays decrease with the initial magnet current, since the conductor magnetic field increases and consequently the margin to quench decreases. For the same reason, delays after triggering the heaters attached to the high-field region of the coil (HF-OL-H) are shorter than after triggering low-field region heaters (LF-OL-H). At nominal current, delays measured in the three magnets are within 9 to 11 ms for HF-OL-H, and 14 to 19 ms for LF-OL-H. In the low to medium current range, MQXFPM1 low-field outer layer heater delays are shorter than expected.

The delays measured after triggering inner layer heaters are plotted in Fig. 2b. At nominal current, delays are in the 8 to 20 ms range.

For both outer and inner layer heaters, the consistency between the delays measured on short and long magnets confirms the good scalability of the heater technology with the magnet length.

Another key heater performance parameter is the minimum heater energy density required to initiate a transition to

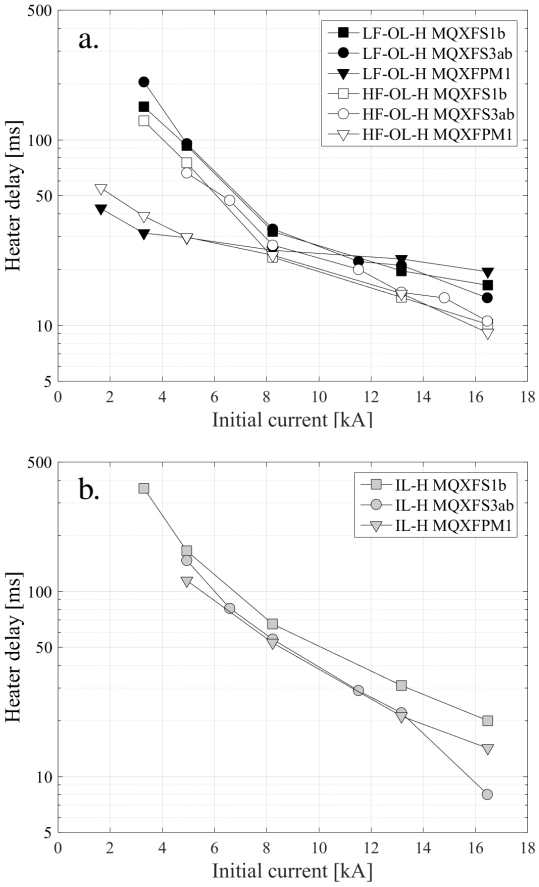

Fig. 2. Measured heater delay as a function of the magnet current [25]–[30]. Tests were performed with the parameters summarized in Table III. a. Heaters attached to the low- (LF-OL-H) and high-field (LF-OL-H) regions of the outer layer. b. Heaters attached to the inner layer (IL-H).

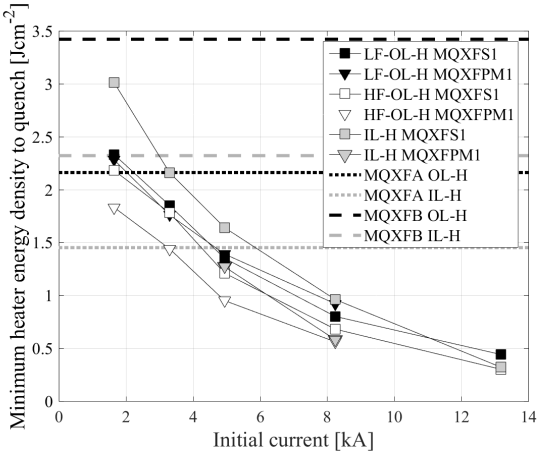

Fig. 3. Measured minimum heater energy density to quench as a function of the magnet current [25], [29], [30], compared to MQXFA (dotted lines) and MQXFB (dashed lines) design values. Capacitances of the heater units used during MQXFS1 and MQXFPM1 tests are 19.2 and 12.4 mF, respectively.

the normal state, $E_{\mathrm{H,min}}$ [Jm^{-2}]. The results of $E_{\mathrm{H,min}}$ tests performed on the MQXFS1 and MQXFPM1 magnets are shown in Fig. 3. It is important to verify that the target deposited energies detailed in Table II are higher than $E_{\mathrm{H,min}}$. This condition is satisfied at all tested current levels by MQXFB targets for HF-OL-H and LF-OL-H. On the contrary, at 10% I_{nom} the MQXFA target is slightly lower than LF-OL-H $E_{\mathrm{H,min}}$. Moreover, the MQXFA and MQXFB target energy densities for IL-H are sufficient to initiate a quench only above about 35% and 20% I_{nom}. However, since transferring a relatively small part of the coil to the normal state is sufficient to protect the magnet at low currents, the overall heater performance is adequate.

Heater long-term reliability is crucial for assuring magnet quench protection during the entire machine life-time, since multiple heater failures could significantly increase the peak magnet voltages to ground and hot-spot temperature [10]. During MQXFS1 and MQXFS3 test campaigns, several cases of heater electrical failures and heater-to-coil detachments occurred in the inner-layer heater strips, which question the implementation of this technology in the high luminosity LHC inner triplet magnets [27].

TABLE IV
MQXF CLIQ PARAMETERS [9], [10].

Parameter	Unit	MQXFA	MQXFB
CLIQ unit charging voltage	V	1000	600
CLIQ unit capacitance	mF	40	40
CLIQ circuit resistance	mΩ	$\leq$100	$\leq$100

B. Coupling-Loss Induced Quench System

Each inner triplet circuit will include six 40 mF CLIQ units for the protection of six magnets [9], [10]. To minimize the spare management effort, all units will be built following the same design, as detailed in Table IV. It has been shown that the peak power density deposited in the strands after triggering CLIQ is roughly proportional to the square of the ratio between the unit charging voltage U_0 [V] and the magnetic length l_{m} [m] [14]. Thus, in order to target the same peak power density the units connected to the shorter magnets will be charged to a lower voltage.

In order to test CLIQ on the short model magnets in conditions more similar to the design targets, a larger capacitance C [F] is required. In fact, the CLIQ oscillation frequency is inversely proportional to $\sqrt{l_{\mathrm{m}}C}$ [14]. Due to hardware limitations the highest available CLIQ capacitance was 80 mF, and thus the oscillation frequency in the first model campaign was almost twice higher than the MQXF design target. As a result CLIQ performance was partly reduced, since the more frequent current polarity changes cause the coupling currents to reset more often, and hence decrease the coupling loss deposited over time.

III. QUENCH PROTECTION SYSTEM PERFORMANCE

Quench protection system induced discharges have been performed on the first two model magnets to assess the performances of different protection configurations including heaters and CLIQ. The conductor parameters of the coils assembled in the MQXFS1 and MQXFS3 magnets are summarized in Table V. Note that two of the four MQXFS1

TABLE V
MAIN CONDUCTOR PARAMETERS OF THE TESTED MQXF SHORT MODEL COILS [7], [8].

Coil	Assembly	Strand type	Cu/no-Cu ratio	RRR[a]	$l_{\mathrm{tp,f}}$ [mm]	$l_{\mathrm{tp,s}}$ [mm]
Specifications	-	-	1.2±0.1	≥100	19±3	109±3
QXFS03	MQXFS01	RRP 108/127	1.165	250	14	109
QXFS104	MQXFS01	RRP 132/169	1.174	105	19	109
QXFS05	MQXFS01	RRP 108/127	1.182	255	14	109
QXFS103	MQXFS01	RRP 132/169	1.174	135	19	109
QXFS07	MQXFS03	RRP 108/127	1.199	170	14	109
QXFS105	MQXFS03	RRP 132/169	1.218	140	19	109
QXFS106	MQXFS03	RRP 132/169	1.218	140	19	109
QXFS107	MQXFS03	RRP 132/169	1.214	140	19	109

[a]RRR measured between 297 K and 20 K.

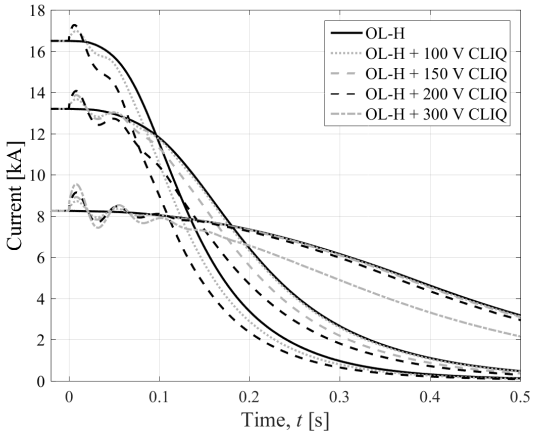

Fig. 4. Comparison between MQXFS1b magnet discharges obtained by triggering outer-layer heaters only, or outer-layer heaters and one CLIQ unit charged to different voltage levels. Measured magnet current I_{m} versus time.

coils include OL-H strips featuring a different design [7], [34], and about half of the IL-H strips of both magnets experienced electrical problems and were not included in the protection scheme [27]. All heater and CLIQ parameters were selected to reproduce the MQXF target design performance as closely as allowed by hardware limitations. In particular, heater and CLIQ unit charging voltages were reduced by a factor roughly proportional to the ratio between the magnetic lengths of MQXFB and the model magnets, i.e. $\approx 7.15/1.19$.

A. Experimental results

Tests were performed on both magnets at different current levels by manually triggering the quench detection system, and hence activating the protection elements. Average triggering times were 0.5 ms for the MQXFS1 heater and CLIQ units, and 4 ms for the MQXFS3 heater units. The currents measured during MQXFS1 magnet discharges for initial currents between 8.2 and 16.5 kA, corresponding to 50% to 100% of nominal current, are plotted in Fig. 4. Discharges obtained by simultaneously triggering outer-layer heaters and one CLIQ unit are compared to those obtained by triggering only OL-H. As expected, adding CLIQ to the protection system improves its performance. OL-H and CLIQ constitute an effective synergy since they are based on different heating mechanisms and deposit energy in different coil regions. In fact, OL-H heat up by thermal diffusion the outer layer, to which they are attached, whereas CLIQ heats up the strands where high magnetic-field changes are introduced, namely the inner layer and the mid-plane turns, utilizing inter-filament coupling loss [21], [22]. Similar discharges were performed for different CLIQ charging voltages to assess its impact on the magnet discharge. At nominal current, the curve obtained for U_0=200 V, which achieves a peak power deposited density similar to the MQXFB target, is significantly faster than that obtained with only OL-H.

A parameter often used to assess the protection system performance is the quench load, defined as the integral of the square of the magnet current during its discharge, $\int {I_{\mathrm{m}}}^2 \mathrm{dt}$ [$\mathrm{A^2s}$]. Its value is roughly proportional to the energy deposited in the coil's hot-spot by joule heating. The quench loads obtained during MQXFS1 discharges in the range 10% to 109% I_{nom}, calculated from the manual quench detection triggering, are shown in Fig. 5a. The current level at which CLIQ effectively reduces the quench load depends on the unit charging voltage. For a 200 V unit, achieving a peak power deposition similar to the MQXFB design target, the quench load is reduced for current levels above 50% I_{nom}. At I_{nom}, the quench load is reduced by more than 20%. For a 300 V unit, achieving a total energy deposition per unit volume similar to the MQXFB target, the quench load is reduced already at 30% I_{nom}. Increasing the unit capacitance would improve the low-current performance. However, the protection in this current range is not critical and can be assured more cost-effectively by OL-H only. Therefore, it is important to assure the OL-H redundancy.

The quench loads obtained in similar tests performed on the MQXFS3 magnet are plotted in Fig. 5b. As one can calculate from the values reported in Table V, the MQXFS3 coil resistance is 1% and 10% higher than MQXFS1 at room temperature and 20 K, respectively. Nonetheless, the quench loads measured during MQXFS3 OL-H tests are higher than MQXFS1. This indicates that MQXFS1 coil is transferred more quickly to the normal state. With respect to the OL-H discharges, a reduction of about 2 $\mathrm{MA^2s}$ was achieved when both OL-H and IL-H were triggered simultaneously.

In the case of a real quench occurring in the magnet, the actual quench loads would be higher due to the additional time required to detect the quench on-start. At nominal current,

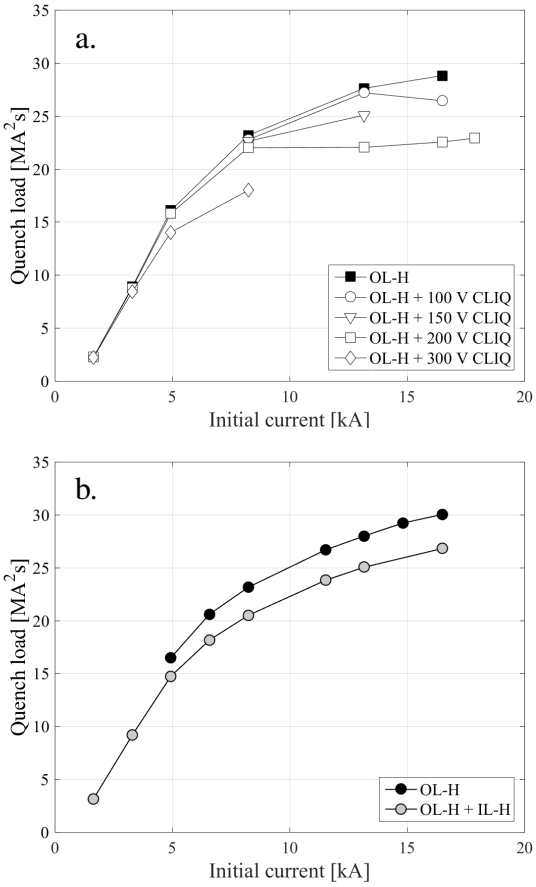

Fig. 5. Calculated quench loads as a function of the magnet current, obtained by triggering various combinations of heaters and CLIQ protection systems. a. MQXFS1 magnet [29], [30]. b. MQXFS3 magnet [26]–[28]. Values are calculated from the manual quench detection triggering. The values at currents below 5 kA are further reduced due to the triggering of a 30 mΩ energy-extraction system, occurring 1 s after quench detection.

assuming a quench detection and validation time of 15 ms, this extra contribution is about 4 MA^{2}s. In these conditions, the expected hot-spot temperature at the end of a discharge from I_{nom} would be about 250 K for the protection configurations including OL-H together with either CLIQ or IL-H, and above 320 K for the OL-H case. Analyses showed that if strand parameter variability is high and/or failure cases occur the configuration including only OL-H is not sufficient to maintain the hot-spot temperature below the target limit of 350 K [10], which is considered a safe limit with respect to permanent degradation [35].

In conclusion, a protection strategy relying both on heaters and CLIQ appears a very good choice in terms of hot-spot temperature reduction, redundancy improvement, and long-term system reliability.

B. Simulation results

The electro-magnetic and thermal transients occurring in the magnets during the tests are simulated with the LEDET program [14], [32], [33]. The comparison between the experimental and simulated quench loads after triggering the protection system at nominal current is shown in Table VI.

TABLE VI
QUENCH LOADS CALCULATED DURING MQXF MODEL MAGNET TESTS AT NOMINAL CURRENT AND COMPARISON WITH MODELING RESULTS.

Magnet	Configuration	Quench load [MA^{2}s]		
		Measurement	Model	Discrepancy
MQXFS1	OL-H	28.8	32.2	+12%
MQXFS1	OL-H + CLIQ	22.5	26.5	+18%
MQXFS3	OL-H	30.0	32.1	+ 7%
MQXFS3	OL-H + IL-H	26.8	27.5	+ 2%

As detailed in the text, heater and CLIQ configurations are not identical to the final design targets. Simulations attempt to reproduce test configurations.

Simulations overestimate the quench load by 2% to 12% for the heater-induced transients, and 18% for the OL-H and CLIQ discharge. Possible explanations for the quench load overestimation are inaccuracies in the material properties, strand parameters, and model assumptions. Several effects might be implemented in the model in an attempt to improve its accuracy, including the resistance developed in the magnet ends, the strain-dependency of the Nb_3Sn critical current, the effect of the strand twist-pitch on the ohmic loss per conductor unit length, the superconductor hysteretic loss, and the temperature gradient within the conductor's metal, epoxy, and insulation volumes.

IV. CONCLUSION

The quench protection system of the Nb_3 quadrupole magnets for the high luminosity LHC upgrade was characterized by assessing the performance of its individual components in short and long magnet models. The protection scheme includes heater strips glued to the coil surfaces and CLIQ units electrically connected to the magnets.

The performances of individual heater strips in terms of delay between triggering and induced transition to the normal state are evaluated for the first two 1.2 m model magnets and one 4.0 m mirror magnet. The measured delays are sufficiently short to provide an effective quench heating. Scalability of the heater technology is successfully demonstrated after measuring similar delays for short and long heater strips. The long-term reliability of heater strips attached to the coil's inner layer is not demonstrated at this time since several cases of electrical failures and heater detachments occurred in the first two model magnets.

The addition of CLIQ units to the protection scheme allows achieving a faster magnet discharge, and hence reducing significantly the hot-spot temperature at the end of the quench transient. Tests performed by charging the CLIQ units at different voltages show that the selected design values are a correct compromise between reducing the hot-spot temperature and reducing the unit charging voltage.

ACKNOWLEDGMENT

The authors wish to thank Bernardo Bordini (CERN), Lance Cooley (FNAL), Dan Dietderich (LBNL), and Ian Pong (LBNL) for their help in tracing the information about MQXF superconductor parameters.

REFERENCES

[1] G. Apollinari, O. Brüning, and L. Rossi, "High Luminosity LHC Project Description," CERN, Geneva, Tech. Rep. CERN-ACC-2014-0321, Dec 2014. [Online]. Available: https://cds.cern.ch/record/1974419

[2] G. Apollinari, I. Béjar Alonso, O. Brüning, M. Lamont, and L. Rossi, *High-Luminosity Large Hadron Collider (HL-LHC): Preliminary Design Report*. Geneva: CERN, 2015. [Online]. Available: http://cds.cern.ch/record/2116337

[3] E. Todesco, H. Allain, G. Ambrosio, G. Arduini, F. Cerutti, R. D. Maria, L. Esposito, S. Fartoukh, P. Ferracin, H. Felice, R. Gupta, R. Kersevan, N. Mokhov, T. Nakamoto, I. Rakno, J. M. Rifflet, L. Rossi, G. L. Sabbi, M. Segreti, F. Toral, Q. Xu, P. Wanderer, and R. van Weelderen, "A first baseline for the magnets in the high luminosity LHC insertion regions," *IEEE Transactions on Applied Superconductivity*, vol. 24, no. 3, pp. 1–5, June 2014.

[4] P. Ferracin, G. Ambrosio, M. Anerella, F. Borgnolutti, R. Bossert, D. Cheng, D. R. Dietderich, H. Felice, A. Ghosh, A. Godeke, S. Izquierdo Bermudez, P. Fessia, S. Krave, M. Juchno, J. C. Perez, L. Oberli, G. Sabbi, E. Todesco, and M. Yu, "Magnet design of the 150 mm aperture low-β quadrupoles for the High Luminosity LHC," *IEEE Transactions on Applied Superconductivity*, vol. 24, no. 3, pp. 1–6, June 2014.

[5] G. Ambrosio, "Nb_3Sn high field magnets for the High Luminosity LHC upgrade project," *IEEE Transactions on Applied Superconductivity*, vol. 25, no. 3, pp. 1–7, June 2015.

[6] E. Todesco, H. Allain, G. Ambrosio, F. Borgnolutti, F. Cerutti, D. Dietderich, L. Esposito, H. Felice, P. Ferracin, G. Sabbi, P. Wanderer, and R. V. Weelderen, "Design studies for the low-beta quadrupoles for the LHC luminosity upgrade," *IEEE Transactions on Applied Superconductivity*, vol. 23, no. 3, pp. 4 002 405–4 002 405, June 2013.

[7] G. Ambrosio, P. Ferracin, and al., "MQXFS1 Quadrupole Design Report," Tech. Rep. FERMILAB-TM-2613-TD, 2016.

[8] L. D. Cooley, A. K. Ghosh, D. R. Dietderich, and I. Pong, "Conductor specification and validation for High-Luminosity LHC quadrupole magnets," *IEEE Transactions on Applied Superconductivity*, vol. 27, no. 4, pp. 1–5, June 2017.

[9] E. Ravaioli, G. Ambrosio, B. Auchmann, P. Ferracin, M. Maciejewski, F. Rodriguez-Mateos, G. Sabbi, E. Todesco, and A. Verweij, "Quench protection system optimization for the High Luminosity LHC Nb_3Sn quadrupoles," *IEEE Transactions on Applied Superconductivity*, vol. PP, no. 99, pp. 1–1, 2017.

[10] E. Ravaioli, "Quench protection studies for the High-Luminosity LHC inner triplet circuit," CERN, Geneva, Tech. Rep. EDMS 1760496, 2016.

[11] G. Manfreda, G. Ambrosio, V. Marinozzi, T. Salmi, M. Sorbi, and G. Volpini, "Quench protection study of the Nb_3Sn low-β quadrupole for the LHC luminosity upgrade," *IEEE Transactions on Applied Superconductivity*, vol. 24, no. 3, pp. 1–5, June 2014.

[12] V. Marinozzi, G. Ambrosio, G. Bellomo, G. Chlachidze, H. Felice, M. Marchevsky, T. Salmi, M. Sorbi, and E. Todesco, "Study of quench protection for the Nb_3Sn low-β quadrupole for the LHC luminosity upgrade (HiLumi-LHC)," *IEEE Transactions on Applied Superconductivity*, vol. 25, no. 3, pp. 1–5, June 2015.

[13] E. Ravaioli, B. Auchmann, V. I. Datskov, J. Blomberg Ghini, K. Dahlerup-Petersen, A. M. Fernandez Navarro, G. Kirby, M. Maciejewski, F. Rodriguez-Mateos, H. H. J. ten Kate, and A. P. Verweij, "Advanced quench protection for the Nb_3Sn quadrupoles for the High Luminosity LHC," *IEEE Transactions on Applied Superconductivity*, vol. 26, no. 3, pp. 1–6, April 2016.

[14] E. Ravaioli, "CLIQ," Ph.D. dissertation, Enschede, 2015, presented on 19 June 2015. [Online]. Available: http://doc.utwente.nl/96069/

[15] V. Datskov, G. Kirby, and E. Ravaioli, "AC-current induced quench protection system," Patent EP13 174 323.9, June 28, 2013.

[16] E. Ravaioli, V. I. Datskov, C. Giloux, G. Kirby, H. H. J. ten Kate, and A. P. Verweij, "New, Coupling Loss Induced, Quench protection system for superconducting accelerator magnets," *IEEE Transactions on Applied Superconductivity*, vol. 24, no. 3, pp. 1–5, June 2014.

[17] A. P. Verweij, "Electrodynamics of superconducting cables in accelerator magnets," Ph.D. dissertation, Twente U., Twente, 1995, presented on 15 Sep 1995. [Online]. Available: https://cds.cern.ch/record/292595

[18] M. Wilson, *Superconducting Magnets*, ser. Monographs on Cryogenics. Clarendon Press, 1983.

[19] E. Ravaioli, V. Datskov, A. Dudarev, G. Kirby, K. Sperin, H. ten Kate, and A. Verweij, "First experience with the new Coupling Loss Induced Quench system," *Cryogenics*, vol. 60, pp. 33–43, 2014. [Online]. Available: http://www.sciencedirect.com/science/article/pii/S0011227514000162

[20] E. Ravaioli, V. I. Datskov, G. Kirby, H. H. J. ten Kate, and A. P. Verweij, "A new hybrid protection system for high-field superconducting magnets," *Superconductor Science and Technology*, vol. 27, no. 4, p. 044023, 2014. [Online]. Available: http://stacks.iop.org/0953-2048/27/i=4/a=044023

[21] E. Ravaioli, H. Bajas, V. I. Datskov, V. Desbiolles, J. Feuvrier, G. Kirby, M. Maciejewski, G. Sabbi, H. H. J. ten Kate, and A. P. Verweij, "Protecting a full-scale Nb_3Sn magnet with CLIQ, the new Coupling-Loss-Induced Quench system," *IEEE Transactions on Applied Superconductivity*, vol. 25, no. 3, pp. 1–5, June 2015.

[22] E. Ravaioli, V. I. Datskov, V. Desbiolles, J. Feuvrier, G. Kirby, M. Maciejewski, K. A. Sperin, H. H. ten Kate, A. P. Verweij, and G. Willering, "Towards an optimized Coupling-loss Induced Quench protection system (CLIQ) for quadrupole magnets," *Physics Procedia*, vol. 67, pp. 215–220, 2015. [Online]. Available: http://www.sciencedirect.com/science/article/pii/S1875389215004186

[23] E. Ravaioli, H. Bajas, V. I. Datskov, V. Desbiolles, J. Feuvrier, G. Kirby, M. Maciejewski, H. H. J. ten Kate, A. P. Verweij, and G. Willering, "First implementation of the CLIQ quench protection system on a full-scale accelerator quadrupole magnet," *IEEE Transactions on Applied Superconductivity*, vol. 26, no. 3, pp. 1–5, April 2016.

[24] E. Ravaioli, V. I. Datskov, G. Dib, A. M. Fernandez Navarro, G. Kirby, M. Maciejewski, H. H. J. ten Kate, A. P. Verweij, and G. Willering, "First implementation of the CLIQ quench protection system on a 14-m-long full-scale LHC dipole magnet," *IEEE Transactions on Applied Superconductivity*, vol. 26, no. 4, pp. 1–5, June 2016.

[25] J. Muratore, M. Anerella, P. Joshi, P. Kovach, A. Marone, and P. Wanderer, "Design and fabrication of the 1.9 K magnet test facility at BNL, and test of the first 4-m-long MQXF coil," *IEEE Transactions on Applied Superconductivity*, vol. 28, no. 3, pp. 1–4, April 2018.

[26] H. Bajas and et al., "Test results of the short models MQXFS3 and MQXFS5 for the HL-LHC upgrade," *IEEE Transactions on Applied Superconductivity*, submitted for publication.

[27] S. Izquierdo Bermudez, G. Ambrosio, H. Bajas, G. Chlachidze, J. F. Troitino, P. Ferracin, E. Ravaioli, S. Stoynev, E. Todesco, G. Sabbi, and G. Vallone, "Overview of the Quench Heater Performance for MQXF, the Nb_3Sn low-β Quadrupole for the High Luminosity LHC," *IEEE Transactions on Applied Superconductivity*, submitted for publication.

[28] S. Izquierdo Bermudez, "Protection studies - HCMQXFM001-CR000032," CERN, Geneva, Tech. Rep. EDMS 1836709, 2017.

[29] G. Chlachidze, G. Ambrosio, M. Anerella, R. Bossert, E. Cavanna, D. W. Cheng, D. R. Dietderich, J. DiMarco, H. Felice, P. Ferracin, A. K. Ghosh, P. Grosclaude, M. Guinchard, A. R. Hafalia, E. F. Holik, S. Izquierdo Bermudez, S. T. Krave, M. Marchevsky, A. Nobrega, D. Orris, H. Pan, J. C. Perez, S. Prestemon, E. Ravaioli, G. Sabbi, T. Salmi, J. Schmalzle, S. E. Stoynev, T. Strauss, C. Sylvester, M. Tartaglia, E. Todesco, G. Vallone, G. Velev, P. Wanderer, X. Wang, and M. Yu, "Performance of the first short model 150-mm-aperture Nb_3Sn quadrupole MQXFS for the High-Luminosity LHC upgrade," *IEEE Transactions on Applied Superconductivity*, vol. 27, no. 4, pp. 1–5, June 2017.

[30] S. Stoynev, G. Ambrosio, M. Anerella, R. Bossert, E. Cavanna, D. Cheng, D. Dietderich, J. DiMarco, H. Felice, P. Ferracin, G. Chlachidze, A. Ghosh, P. Grosclaude, M. Guinchard, A. R. Hafalia, E. F. Holik, S. I. Bermudez, S. Krave, M. Marchevsky, A. Nobrega, D. Orris, H. Pan, J. C. Perez, S. Prestemon, E. Ravaioli, G. Sabbi, T. Salmi, J. Schmalzle, T. Strauss, C. Sylvester, M. Tartaglia, E. Todesco, G. Vallone, G. Velev, P. Wanderer, X. Wang, and M. Yu, "Summary of test results of MQXFS1 - the first short model 150 mm aperture Nb_3Sn quadrupole for the high-luminosity lhc upgrade," *IEEE Transactions on Applied Superconductivity*, vol. 28, no. 3, pp. 1–5, April 2018.

[31] G. Ambrosio, G. Chlachidze, P. Wanderer, P. Ferracin, and G. Sabbi, "First Test Results of the 150 mm Aperture IR Quadrupole Models for the High Luminosity LHC," in *2nd North American Particle Accelerator Conference (NAPAC2016) Chicago, Illinois, USA, October 9-14, 2016*, 2016. [Online]. Available: http://lss.fnal.gov/archive/2016/conf/fermilab-conf-16-440-td.pdf

[32] E. Ravaioli, B. Auchmann, M. Maciejewski, H. ten Kate, and A. Verweij, "Lumped-element dynamic electro-thermal model of a superconducting magnet," *Cryogenics*, pp. –, 2016. [Online]. Available: http://www.sciencedirect.com/science/article/pii/S0011227516300832

[33] E. Ravaioli, B. Auchmann, G. Chlachidze, M. Maciejewski, G. Sabbi, S. E. Stoynev, and A. Verweij, "Modeling of inter-filament coupling currents and their effect on magnet quench protection," *IEEE Transactions on Applied Superconductivity*, vol. 27, no. 4, pp. 1–8, June 2017.

[34] G. Ambrosio and al., "MQXFS1 Quadrupole Fabrication Report," Tech. Rep. LARP DocDB 1117, 2016.

[35] G. Ambrosio, "Maximum allowable temperature during quench in Nb_3Sn accelerator magnets," in *Proceedings, WAMSDO 2013 Workshop on Accelerator Magnet, Superconductor, Design and Optimization: CERN Geneva, Switzerland, 15-16 Jan 2013*, no. FERMILAB-CONF-13-593-TD, 2013, pp. 43–46. [Online]. Available: https://inspirehep.net/record/1277941/files/arXiv:1401.3955.pdf